



Universidad Autónoma  
de Madrid

**Biblos-e Archivo**  
Repositorio Institucional UAM

Repositorio Institucional de la Universidad Autónoma de Madrid  
<https://repositorio.uam.es>

Esta es la **versión de autor** del artículo publicado en:  
This is an **author produced version** of a paper published in:

Applied Catalysis B: Environmental 281 (2021): 119469

DOI: <https://doi.org/10.1016/j.apcatb.2020.119469>

**Copyright:** © 2021 Elsevier Ltd. This manuscript version is made available under the CC-BY-NC-ND 4.0 licence <http://creativecommons.org/licenses/by-nc-nd/4.0/>

El acceso a la versión del editor puede requerir la suscripción del recurso  
Access to the published version may require subscription

This is an electronic reprint of the original article. This reprint may differ from the original in pagination and typographic detail.

---

## Enhanced H<sub>2</sub> production in the aqueous-phase reforming of maltose by feedstock pre-hydrogenation

Oliveira, A. S.; Aho, A.; Baeza, J. A.; Calvo, L.; Simakova, I. L.; Gilarranz, M. A.; Murzin, D. Yu

*Published in:*  
Applied Catalysis B: Environmental

*DOI:*  
[10.1016/j.apcatb.2020.119469](https://doi.org/10.1016/j.apcatb.2020.119469)

Published: 01/02/2021

*Document Version*  
Accepted author manuscript

*Document License*  
CC BY-NC-ND

[Link to publication](#)

*Please cite the original version:*

Oliveira, A. S., Aho, A., Baeza, J. A., Calvo, L., Simakova, I. L., Gilarranz, M. A., & Murzin, D. Y. (2021). Enhanced H<sub>2</sub> production in the aqueous-phase reforming of maltose by feedstock pre-hydrogenation. *Applied Catalysis B: Environmental*, 281, Article 119469. <https://doi.org/10.1016/j.apcatb.2020.119469>

### General rights

Copyright and moral rights for the publications made accessible in the public portal are retained by the authors and/or other copyright owners and it is a condition of accessing publications that users recognise and abide by the legal requirements associated with these rights.

### Take down policy

If you believe that this document breaches copyright please contact us providing details, and we will remove access to the work immediately and investigate your claim.

# Enhanced H<sub>2</sub> production in the aqueous-phase reforming of maltose by feedstock pre-hydrogenation

A. S. Oliveira<sup>a</sup>, A. Aho<sup>b</sup>, J. A. Baeza<sup>a</sup>, L. Calvo<sup>a</sup>, I. L. Simakova<sup>c</sup>, M. A. Gilarranz<sup>a</sup>,  
D. Yu. Murzin<sup>b\*</sup>

<sup>a</sup>Departamento de Ingeniería Química, C/Francisco Tomás y Valiente 7, Universidad Autónoma de Madrid, 28049 Madrid, Spain

<sup>b</sup>Laboratory of Industrial Chemistry and Reaction Engineering, Process Chemistry Centre, Åbo Akademi University, 20500, Turku/Åbo, Finland

<sup>c</sup>Borshkov Institute of Catalysis, 630090 Novosibirsk, Russia

\*corresponding author e-mail: dmitry.murzin@abo.fi

## Abstract

Coupled hydrogenation and aqueous-phase reforming (APR) was studied as an approach to enhance H<sub>2</sub> production from brewery wastewater, where maltose is the main component. Hydrogenation of maltose-bearing wastewater produced essentially maltitol. APR stage was performed over PtPd/C catalysts. Faster catalyst deactivation was observed in the APR of maltose than in the APR of maltitol, especially at high feedstock concentration. Higher H<sub>2</sub> selectivity and yield were achieved in the APR of maltitol. The increase of temperature from 175 to 225 °C changed the reaction pathways, favouring the production of C1-C2 alkanes for both feedstocks. Higher selectivity to liquid-phase products was obtained in the APR of maltose, evidencing also reaction routes favouring the formation of solid carbonaceous deposits that lead to higher catalyst deactivation. The coupled process can be considered as efficient since H<sub>2</sub> production compensated for H<sub>2</sub> consumption in the hydrogenation stage and catalyst durability was increased.

**Keywords:** hydrogen, aqueous-phase reforming, hydrogenation, brewery wastewater, maltose

## 1. Introduction

Aqueous-phase reforming (APR) is a potential route for the valorisation of organic compounds to gaseous fuels such as  $H_2$  [1]. Important efforts have been made in the application of APR to biorefinery products and side streams [2,3]. Moreover, some studies have shown that biomass-derived organic compounds in wastewaters can also be suitable feedstocks for APR, with sugars as particularly relevant components of wastewater from food and beverage industries [4–6]. In the APR of brewery wastewater, promising results have been also achieved in terms of organic matter removal and  $H_2$  production, with  $H_2$  yield significantly higher than for the anaerobic digestion (12.2 mmol  $H_2$ /g chemical oxygen demand ( $COD_{initial}$ ) [4]. APR of cheese whey also showed a high  $H_2$  yield, similar to that obtained in anaerobic fermentation (4 mol  $H_2$ /mol lactose) [5]. The valorisation of waste compounds contained in wastewater is one of the strong points of this new approach, since techno-economic studies on  $H_2$  production by APR have shown that the feedstock may contribute largely to the production costs [7].

The concentration of organic matter in wastewaters is generally lower than the biorefinery feedstocks usually considered in APR, which could have a significant influence on the catalytic performance. In the APR of brewery wastewater, at low wastewater concentration (1531 mg of  $COD_{initial}$  /L) ca. 99 % of the organic matter was removed giving  $H_2$  yield of 15.4 mmol  $H_2$ /g  $COD_{initial}$ , while at higher concentration (11204 mg of  $COD_{initial}$  /L) these values decreased to 51 % and 7.3 mmol  $H_2$ /g  $COD_{initial}$ , respectively [4]. In the APR of sugars, a higher  $H_2$  selectivity was observed when feedstocks with lower glucose concentrations were used [1]. This is consistent with a lower rate of side reactions to form liquid phase products, such as organic acids and aldehydes, which are less favoured at low sugar concentration [8,9]. However, the use of diluted solutions might not be economically attractive, requiring high energy input to reach the reaction

1 temperature (up to 250 °C). Nevertheless, in the case of wastewaters a higher margin for  
2 operating at lower concentration of organic matter can be expected because APR would  
3 be integrated in the waste management scheme, where higher energy inputs may be more  
4 affordable.

5 Otherwise, the potential of sugar-based feedstocks and wastewaters in the APR can be  
6 hampered by reactions involving aldehyde and ketone groups of sugars that lead to  
7 catalyst deactivation [10], mostly by formation of carbonaceous deposits on the catalysts  
8 surface [8]. In addition, lower H<sub>2</sub> yields and selectivity have been reported in the APR of  
9 sugars, such as glucose, than in the APR of polyols and sugar alcohols (sorbitol, glycerol,  
10 ethylene glycol) [1,9]. Therefore, a strategy to improve H<sub>2</sub> production in sugar-based  
11 feedstocks can be a combination of hydrogenation with APR. Thus, in the hydrogenation  
12 stage, sugars can be converted to more reduced compounds, which react more selectively  
13 to H<sub>2</sub> and CO<sub>2</sub> in the APR stage. In this context, Davda and Dumesic [9] performed a  
14 study that combined hydrogenation and APR of glucose. They observed that after  
15 hydrogenation of glucose to sorbitol in a first step, a high H<sub>2</sub> selectivity (62.4 %) was  
16 achieved and the production of H<sub>2</sub> was ca. 3 fold higher than for direct APR of glucose.  
17 Irmak *et al.* [11] also performed hydrogenation of glucose and biomass hydrolysates  
18 before APR and reported a significantly higher H<sub>2</sub> yield and selectivity than for non-  
19 hydrogenated solutions. Godina *et al.* [12] also combined hydrogenation and APR to  
20 produce hydrogen from commercial sucrose. Thus, hydrogenation of key components  
21 before APR can be an alternative to reduce undesirable reactions and improve H<sub>2</sub>  
22 production. Even if some H<sub>2</sub> is consumed in the hydrogenation of the feedstocks, it can  
23 be compensated by a higher overall net H<sub>2</sub> production. Likewise, hydrogenation can  
24 facilitate the use of solutions with a higher concentration and diminish deactivation of the  
25 catalysts.

This work aims to contribute to knowledge and understanding on the processability by APR of diluted feedstocks based on sugars. Hydrogenation of maltose has been evaluated as an approach to increase suitability of brewery wastewater as a feedstock for APR and H<sub>2</sub> production. Maltose has been chosen as a model compound because it is the main substance component, amounting for ca. 50 wt. % of the organic components in brewery wastewaters, which also include sugars, soluble starch, yeast, ethanol, and volatile fatty acids as other components [13,14]. On the other hand, brewery wastewater has a large potential for valorisation by APR taking into account that the brewing industry generates large volumes of wastewaters (3-10 L wastewater/L beer) [14] with a high organic load ranging from 2000 to 32500 mg of COD/L [15].

## **2. Experimental**

### **2.1. Preparation and characterization of support and catalyst**

A PtPd/C catalyst was used in the APR experiments, since Pt and Pd catalysts have exhibited high selectivity for H<sub>2</sub> production and low selectivity for alkane production [16]. On the other hand, PtPd catalysts have shown to be twice more selective for H<sub>2</sub> production than Pt catalyst in the APR of glycerol, using carbon nanotubes as a support [17]. The PtPd/C catalyst (2.5 wt. % Pt and 1.25 wt. % Pd) was prepared by incipient wetness impregnation using PdCl<sub>2</sub> (Kraszvetmet, Krasnoyarsk, Russia) and H<sub>2</sub>PtCl<sub>6</sub> (Kraszvetmet, Krasnoyarsk, Russia) as metals precursors and a mesoporous carbon Sibunit, developed at the Omsk centre of new chemical technologies of Boreskov Institute of Catalysis, as a support. After co-impregnation of the metal precursors, the catalysts were dried overnight at 110 °C, and then gently reduced starting from the room temperature to 400 °C under H<sub>2</sub> flow (40 N mL/min) with a temperature

1 ramp 2°C/min. Thereafter, the catalyst was additionally treated with H<sub>2</sub> at 400 °C for 3 h  
2 to remove the excess of chloride.

3 The catalyst was characterized by CO chemisorption yielding apparent metal dispersion  
4 and nanoparticle mean size values of 51.6 % and 2.2 nm, respectively, for both metals.

5 The used catalysts were characterized by thermogravimetric analysis (TG) (SDT 650, TA  
6 Instruments). The temperature-programmed desorption (TG-TPD) analysis was  
7 performed at 450 °C for 30 min (10 °C/min heating rate) using a continuous flow of N<sub>2</sub>  
8 (50 N mL/min). Thereafter, the sample was cooled to room temperature and then the flow  
9 was changed to air for the temperature-programmed oxidation (TG-TPO) which was  
10 performed at 550 °C for 2 h (5 °C/min heating rate).

## 11 **2.2. Hydrogenation of maltose**

12 Hydrogenation of the aqueous maltose solution (2.5 wt. %) was performed in a batch  
13 reactor (300 mL, Hasteloy) at 120 °C and 20 bar of H<sub>2</sub> [18]. In this reaction, a commercial  
14 4.6 wt. % Ru catalyst supported on activated carbon was used. The details of the catalyst  
15 including characterization data can be found in a previous work [19]. Maltose of 98 %  
16 purity was purchased from Alfa Aesar. The maltose solution (100 mL) and the catalyst  
17 (0.2 g) were loaded and the reactor was purged several times with Ar before heating up,  
18 stirring (1000 rpm) and pressurizing with H<sub>2</sub>. At the beginning of the reaction, the liquid  
19 samples (2.5 mL) were taken at least every 15 min and then every 30 min until the reaction  
20 was stopped after 2 h. The initial liquid feedstock and liquid samples were analysed by  
21 HPLC (Aminex HPX-87H, RI detector, 45 °C, 5 mM H<sub>2</sub>SO<sub>4</sub>, isocratic conditions, 0.6  
22 mL/min).

## 23 **2.3. Aqueous-phase reforming experiments**

The APR experiments were carried out at 175, 200 and 225 °C, 30 bar of N<sub>2</sub> (1 % He) with 0.5 g of catalyst using a continuous fixed bed reactor equipped with temperature and pressure controllers. The details on the experimental set-up can be found in previous works [20,21]. The reactor was heated externally and the reaction temperature was monitored using a thermocouple placed outside the stainless-steel reactor tube (520 x 6.4 mm) next to the position of catalyst bed. The catalyst bed consisted of a mixture of the catalyst (0.5 g) and sand (3 g) placed in the middle of the reactor tube between two layers of sand (3.5 g above and 4.5 below). In addition to the reduction performed during the synthesis (see procedure above), the catalyst was reduced in situ during 2 h before the APR experiments using a temperature of 250 °C and a H<sub>2</sub> flow rate of 40 N mL/min. Such conditions, as confirmed by temperature programmed reduction (not shown), are sufficient to reduce minor amounts of surface oxides formed in the catalyst during storage.

The APR experiments were started at a temperature of 175 °C, which was raised to 200 °C after 24 h time-on-stream (TOS) and to 225 °C after additional 24 h. Aqueous solutions containing 1 and 2.5 wt. % of model compounds were used in the experiments. The feedstocks were fed into the reactor with a HPLC pump using 0.1 mL/min of the liquid flow rate. The weight-hour space velocities (*WHSV*), calculated as mass of the substrate per hour divided by the mass of catalyst, were 0.12 h<sup>-1</sup> and 0.3 h<sup>-1</sup> for 1 and 2.5 % solutions, respectively. A constant N<sub>2</sub> flow rate 34 N mL/min containing 1 % He was used to purge the reaction system, to maintain the pressure inside the reactor, and as a carrier gas. The gas produced was analysed online by a Micro-Gas chromatograph (Agilent Micro-GC 3000A) equipped with four columns. H<sub>2</sub>, CO, CO<sub>2</sub> and C1-C7 alkanes were detected in the gas produced. The initial feedstocks and the liquid effluents were



analysed by HPLC following the same procedure previously applied for hydrogenation samples.

Equations 1 to 7 were used to quantify the results of experiments and define performance parameters. Conversion of single compounds was calculated as Equation 1:

$$Conversion (\%) = \frac{FC_{initial} - FC_{final}}{FC_{initial}} \times 100 \quad (1)$$

where  $FC$  is the feed concentration in the initial feedstock ( $FC_{initial}$ ) and final effluent ( $FC_{final}$ ) in mol/L.

Carbon conversion to gas ( $CC_{gas}$ ) was calculated according to Equation 2:

$$CC_{gas} (\%) = \frac{C_{gas}}{C_{initial}} \times 100 \quad (2)$$

where  $C_{gas}$  is the total molar carbon flow detected in all gas phase products ( $CO_2$  and alkanes) in mol C/min and  $C_{initial}$  is the molar carbon flow in the initial feedstock (mol C/min).

The  $H_2$  selectivity and yield were calculated by Equations (3) and (4), respectively:

$$Selectivity_{H_2} (\%) = \frac{H_{2gas} \times 2}{total\ of\ hydrogen\ in\ the\ gas\ phase\ products} \times 100 \quad (3)$$

$$Yield_{H_2} (\%) = \frac{H_{2gas}}{H_{2stoichiometric}} \times 100 \quad (4)$$

where  $H_{2gas}$  is the molar flow of  $H_2$  in the gas phase (mol/min) and  $H_{2stoichiometric}$  is the amount of  $H_2$  (mol/min) that would ideally be obtained from the stoichiometric conversion of the feedstock to  $H_2$  and  $CO_2$ . The total amount of hydrogen in the gas phase products was calculated as a sum of each identified product molar flow multiplied by the number of hydrogen atoms in the respective molecule.

For selectivity to CO<sub>2</sub> and alkanes the Equation (5) was used:

$$Selectivity_j (\%) = \frac{C_{j_{gas}}}{C_{gas}} \times 100 \quad (5)$$

where  $C_{j_{gas}}$  is the amount of carbon in a product  $j$  in the gas phase, in mol C/min.

The yield of liquid products was determined by Equation (6):

$$Yield_j (\%) = \frac{C_{j_{liq}}}{C_{initial}} \times 100 \quad (6)$$

where  $C_{j_{liq}}$  is the amount of carbon in a product  $j$  in the liquid phase, in mol C/min.

Turnover frequency for H<sub>2</sub> production ( $TOF_{H_2}$ ) was calculated taking into account contribution of both metals in the following way:

$$TOF_{H_2} (min^{-1}) = \frac{H_{2_{gas}}}{MD \times m_{cat} \times (\frac{ML_{Pt}}{MM_{Pt}} + \frac{ML_{Pd}}{MM_{Pd}})} \quad (7)$$

where  $MD$  is the apparent metal dispersion of both metals (Pt and Pd) obtained from CO chemisorption analysis,  $m_{cat}$  is the mass of catalyst,  $ML_{Pt}$  is the Pt loading,  $ML_{Pd}$  is the Pd loading,  $MM_{Pt}$  is the molar mass of Pt and  $MM_{Pd}$  is the molar mass of Pd.

### 3. Results and Discussion

#### 3.1. Hydrogenation of maltose

The reaction scheme for maltose hydrogenation is represented in Figure 1. It is characterized by formation of maltitol as the main product and other side products such as glucose and sorbitol [18].

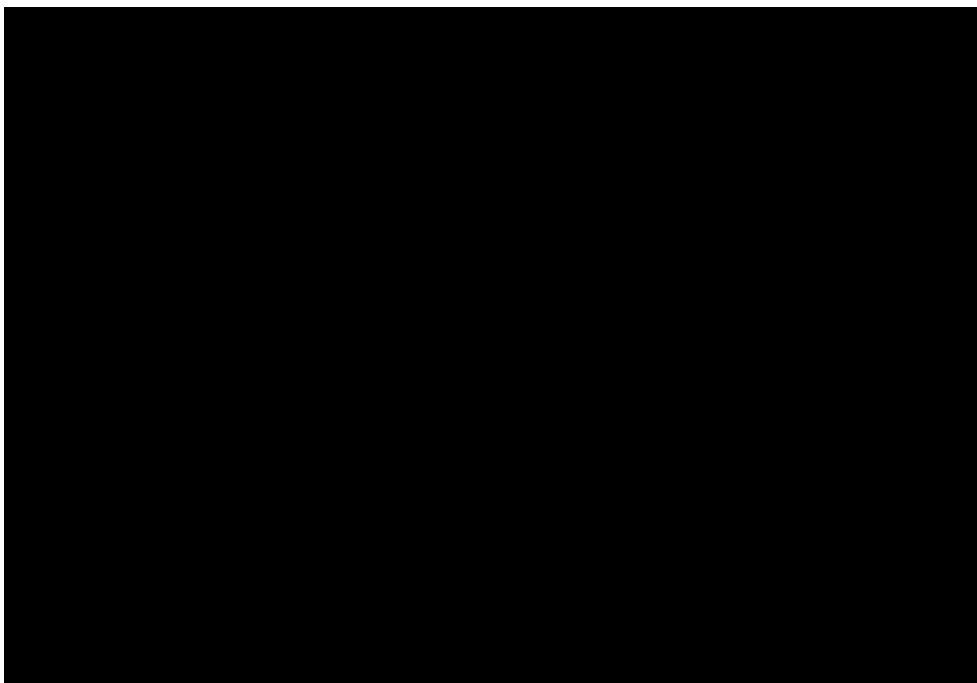


Figure 1. Scheme of maltose hydrogenation (adapted from [18])

The evolution of maltose and maltitol concentration with time during the hydrogenation experiments is showed in Figure 2. After 2 h of reaction, maltose conversion of 99.6 % was obtained, with a maltitol yield of 94.1 % (wt.). Sorbitol was also identified in the liquid phase resulting in a yield of 1.2 % (wt.) after 2 h of reaction, while glucose was not detected in the final effluent under the reaction conditions used. Traces of acids, such as acetic, formic and lactic, were also identified in the liquid phase. These acids can be formed through intermediate hydroxymethylfurfural (HMF), which can be formed by glucose dehydration [22]. Finally, the carbon mass balance closure was 95.7 wt. %. These results show that quantitative hydrogenation of maltose can be achieved and that maltitol can be considered as the main component to be processed in the subsequent APR stage.

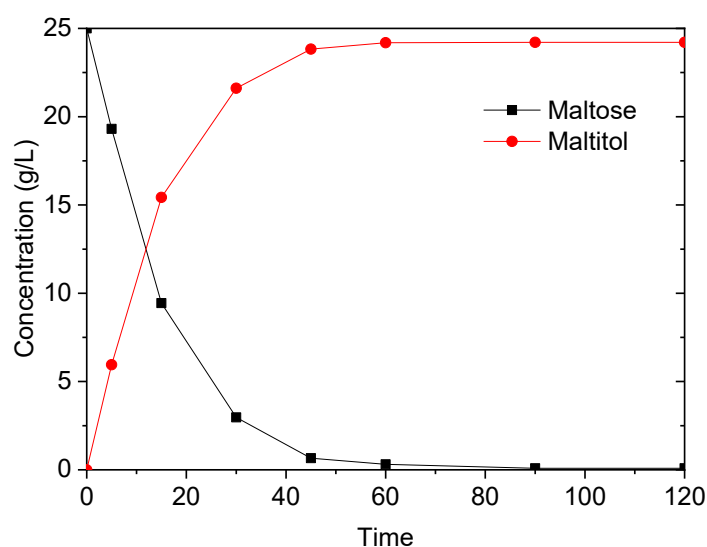


Figure 2. Concentration dependencies of maltose and maltitol with time during hydrogenation (reaction conditions: 120 °C, 20 bar of H<sub>2</sub>, 2 h of reaction, 100 mL of 2.5 % maltose solution, 0.2 g of 4.6 wt. % Ru/C catalyst, 1000 rpm)

## 3.2. APR of maltose and maltitol

### 3.2.1. Time-on-stream behaviour

APR experiments were conducted using 1 and 2.5 wt. % aqueous solutions of maltitol (Alfa Aesar, 95 %). The APR of maltose was also studied at the same conditions for comparison. As indicated above, the experiments were started at 175 °C, and continued at 200 °C and 225 °C. At each temperature, a stabilization period of 1 – 6 h TOS was needed until the conversion and gas production remained stable. Experiments were performed for up to 72 h TOS without significant deactivation or increase of pressure in the reactor, for both 1 and 2.5 % maltitol (Figure 3).

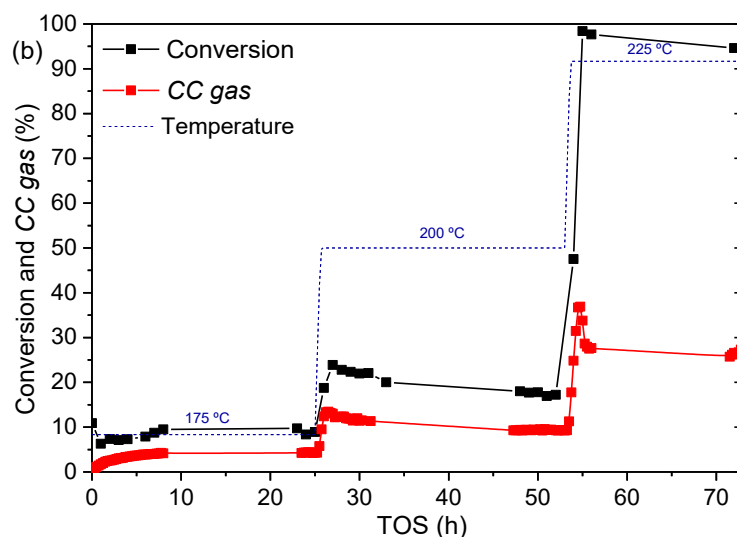
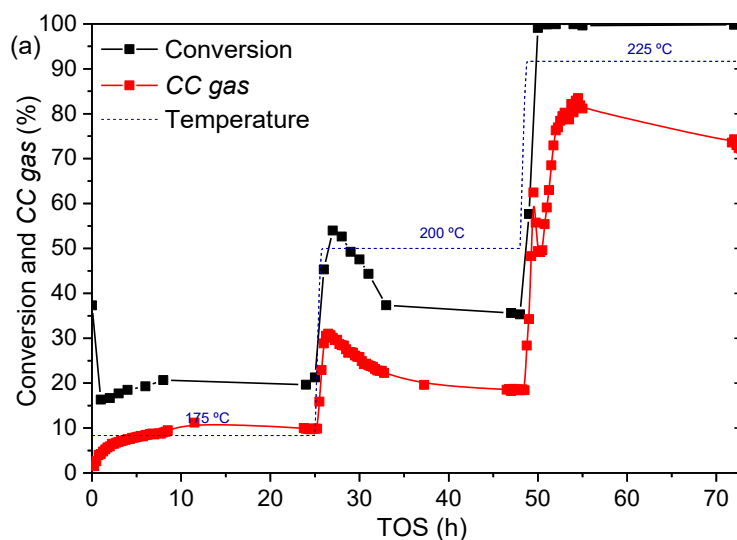


Figure 3. Conversion and *CC gas* in APR of (a) 1 and (b) 2.5 % maltitol (reaction conditions: 30 bar, 0.5 g of PtPd/C catalyst,  $WHSV = 0.12$  and  $0.3 \text{ h}^{-1}$ )

In the APR experiments with maltose solutions (Figure 4), the catalyst showed a significant deactivation after 48 h TOS. Deactivation was more evident when the temperature was raised to 225 °C, even for maltose concentration of 1 %. Likewise, a significant increase in the reactor pressure was observed after 56 h TOS in the case of experiments with 2.5 % maltose, and after 60 h TOS in the case of experiments with 1 % maltose. The rise in pressure may be ascribed to the formation of carbonaceous deposits

inside the reactor and could also be responsible for deactivation observed earlier [9]. The side reactions would be less favoured in the APR of maltitol, which is typical for polyols in comparison to sugars. In addition, these side reactions seem to be favoured at higher temperatures and for more concentrated feedstock solutions, since the experiment with 2.5 % maltose at 225 °C could only be carried out during 8 h TOS, while with 1 % maltose at the same temperature an increase of pressure happened after 12 h TOS.

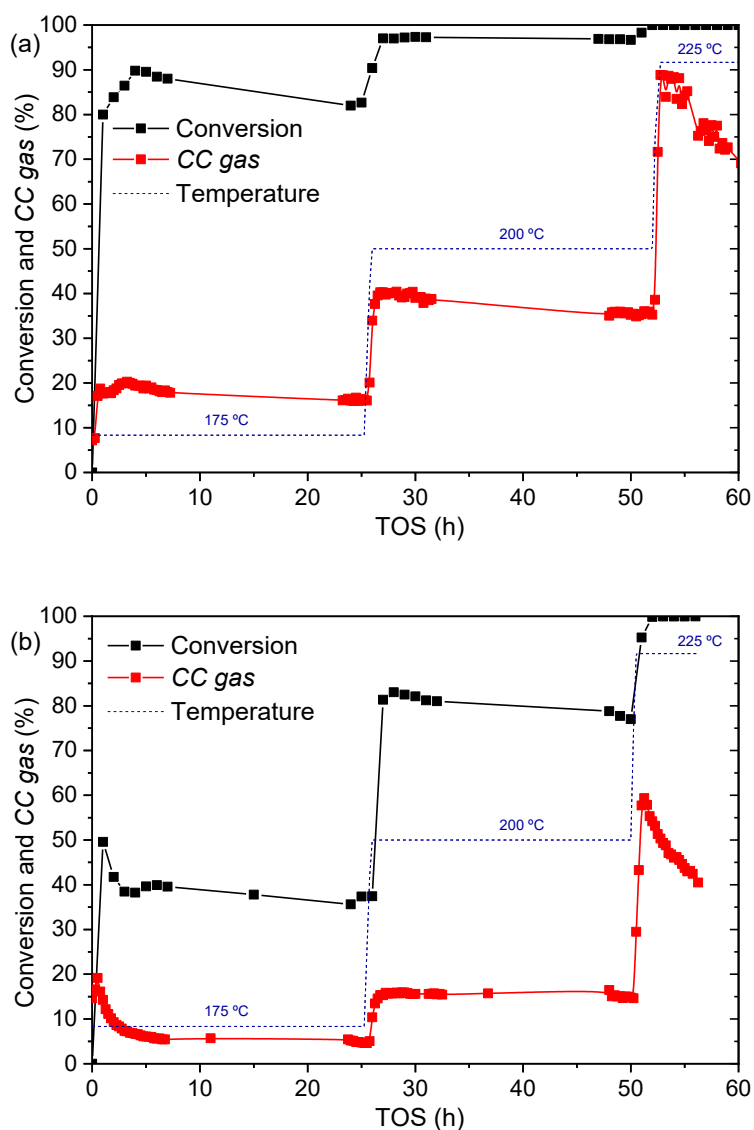


Figure 4. Conversion and *CC gas* in APR of (a) 1 and (b) 2.5 % maltose (reaction conditions: 30 bar, 0.5 g of PtPd/C catalyst,  $WHSV = 0.12$  and  $0.3 \text{ h}^{-1}$ )

### 3.2.2. Catalytic performance

The performance parameters for the APR of maltose and maltitol after catalyst stabilization (average of the stable period) are discussed below. For the APR of maltose at 225 °C, where some deactivation was observed, the results are given as average values within the TOS tested. Conversion of the initial feedstock at different temperatures is shown in Figure 5. As can be seen, APR of maltose led to higher conversion values than APR of maltitol, especially at lower temperatures. In addition, the conversion values increased with increasing temperature and decreased with increasing concentration of the initial feedstock. Pipitone *et al.* [2] also reported that the conversion of glucose and xylose in APR was significantly higher than the conversion of sorbitol and xylitol at 230-270 °C, and that differences were more evident at high temperature. Thus, at 175 °C and using 1 % maltitol, the conversion was 18.4 % and this value decreased to 8.3 % using 2.5 % maltitol. At the same temperature, the conversion of maltose was 86.4 and 38.2 % using 1 and 2.5 %, respectively. When the temperature was increased to 225 °C, both substrates showed very high conversion values, well above 94.5 %.

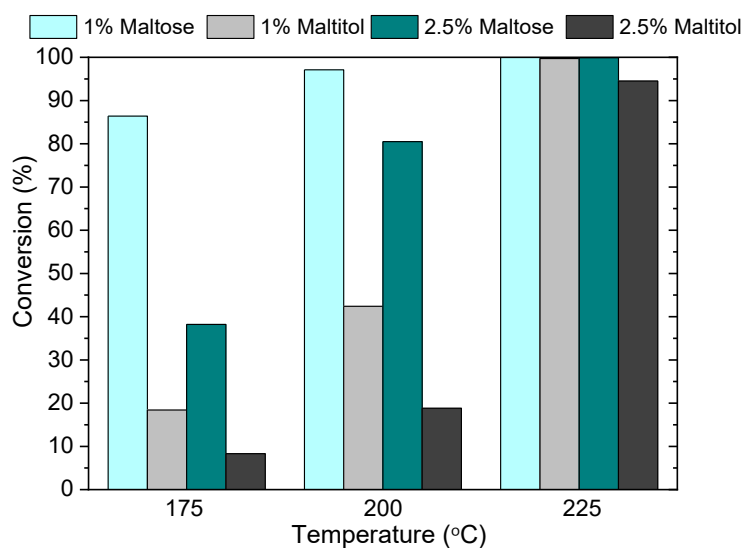


Figure 5. Conversion of maltose and maltitol in APR at different temperatures and initial concentration (reaction conditions: 30 bar, 0.5 g of PtPd/C catalyst,  $WHSV = 0.12$  and  $0.3 \text{ h}^{-1}$ )

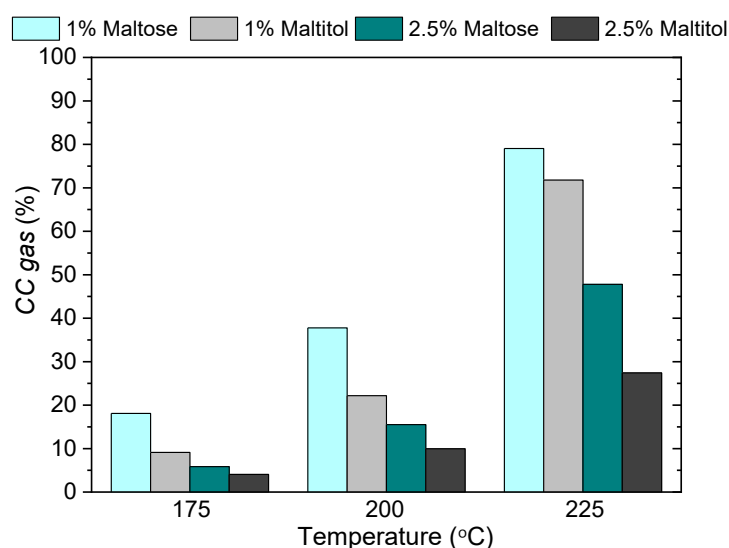


Figure 6. *CC gas* in the APR of maltose and maltitol at different temperatures and initial concentration (reaction conditions: 30 bar, 0.5 g of PtPd/C catalyst,  $WHSV = 0.12$  and  $0.3 \text{ h}^{-1}$ )

Figure 7 shows selectivity to  $\text{H}_2$ ,  $\text{CO}_2$  and alkanes at different temperatures. The selectivity to alkanes was calculated considering all identified hydrocarbons, i.e.  $\text{CH}_4$ ,  $\text{C}_2\text{H}_6$ ,  $\text{C}_3\text{H}_8$ ,  $n\text{-C}_4\text{H}_{10}$ ,  $\text{iso-C}_4\text{H}_{10}$ ,  $n\text{-C}_5\text{H}_{12}$ ,  $\text{iso-C}_5\text{H}_{12}$ ,  $\text{neo-C}_5\text{H}_{12}$ ,  $n\text{-C}_6\text{H}_{14}$ ,  $\text{iso-C}_6\text{H}_{14}$ ,  $\text{C}_6\text{H}_{12}$  and  $n\text{-C}_7\text{H}_{16}$ . APR of maltose was more selective to alkanes than APR of maltitol. Selectivity to alkanes in the reactions with maltose varied from 23.5 to 37.7 %, being between 14.9 and 23.2 % for the reactions with maltitol. Accordingly, selectivity to  $\text{H}_2$



1 was higher in the APR of maltitol (68.7 – 84.2 %) than in the APR of maltose (30.3 –  
2 64.0 %). Davda and Dumesic [9] also reported that H<sub>2</sub> selectivity increased from 13.4 to  
3 62.4 % and alkanes selectivity decreased from 47.5 to 21.3 % by combining  
4 hydrogenation and APR of glucose, where the main hydrogenation product was sorbitol.  
5 Pipitone *et al.* [2] also observed that APR of sorbitol and xylitol was more selective for  
6 H<sub>2</sub> production than APR of glucose and xylose, while Irmak *et al.* [11] reported that in  
7 the APR of glucose and biomass hydrolysate the more reduced feedstocks produced  
8 significantly higher H<sub>2</sub> selectivity and yield than the non-reduced forms.

9 In the APR of both maltose and maltitol the H<sub>2</sub> selectivity decreased when the solution  
10 concentration increased from 1 to 2.5 %, although this effect was more pronounced in the  
11 case of maltose, probably due to a higher contribution of undesired side reactions to form  
12 liquids products and carbonaceous deposits [9]. This decrease in H<sub>2</sub> selectivity was  
13 followed by an increase in alkanes selectivity, which was more pronounced at the highest  
14 temperature.

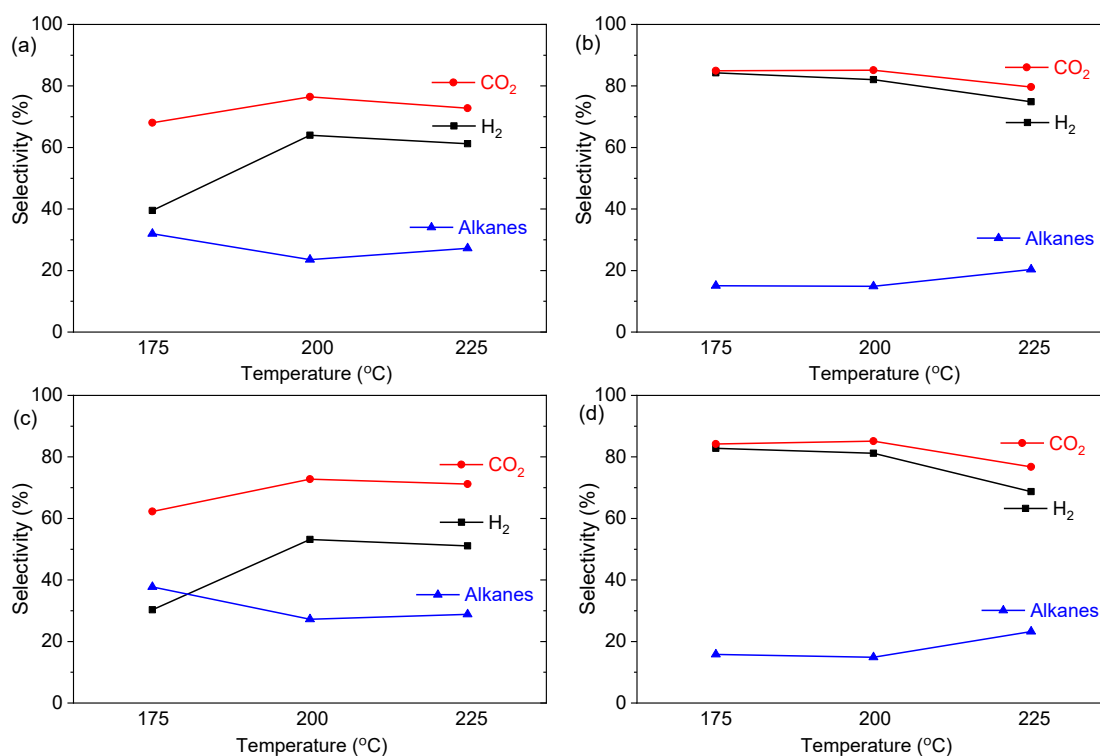


Figure 7. H<sub>2</sub>, CO<sub>2</sub> and alkanes selectivity in APR of (a) 1 % maltose, (b) 1 % maltitol, (c) 2.5 % maltose and (d) 2.5 % maltitol at different temperatures (reaction conditions: 30 bar, 0.5 g of PtPd/C catalyst,  $WHSV = 0.12$  and  $0.3 \text{ h}^{-1}$ )

A more detailed speciation of alkanes is provided in Figure 8, where the identified hydrocarbons were grouped according to the chain length, from C1 to C7. APR of maltose at 175 °C was mainly selective to C5, achieving up to 24.3 % of selectivity to this alkane when a 2.5 % initial concentration was used (Figure 8 (c)). The C5 selectivity significantly decreased with increasing temperature and at 225 °C the selectivity to C5 reached a maximum of 1.3 % (Figure 8 (a) and (c)). The APR of maltitol also showed a maximum of C5 selectivity at 175 °C, although the values were significantly lower than for the APR of maltose (Figure 8 (b) and (d)). C5 alkanes could be formed from consecutive dehydration/hydrogenation and/or dehydrogenation/decarbonylation steps of intermediate compounds present in the liquid phase with C5-C6 atoms [7]. The increase

1 in temperature and initial feedstock conversion favoured selectivity to short chain alkanes  
2 for both maltose and maltitol, and at 225 °C the APR of maltose was more selective to C2  
3 while the APR of maltitol was more selective to C1. In addition, at all the studies  
4 temperatures, the initial feedstock concentration and conversion, the APR of maltitol was  
5 more selective to C1 than to other alkanes. These results indicate that the increase of the  
6 temperature and the use of more reduced compounds changed the reaction pathways,  
7 favouring the fragmentation of the initial feedstock through C-C and C-O bond cleavages  
8 [23], producing short chain alkanes. Similar global alkanes selectivity was observed in  
9 the APR of xylitol using PtRe/C catalyst, although the selectivity to a particular alkane  
10 displayed large variations with the metallic active phase used [20]. On the other hand, in  
11 the APR of sorbitol, a high selectivity to C1 and C2 alkanes was observed using PtPd/C  
12 catalyst [24]. A higher alkanes selectivity was also achieved for monometallic Pd  
13 catalysts than for Pt catalysts [25]

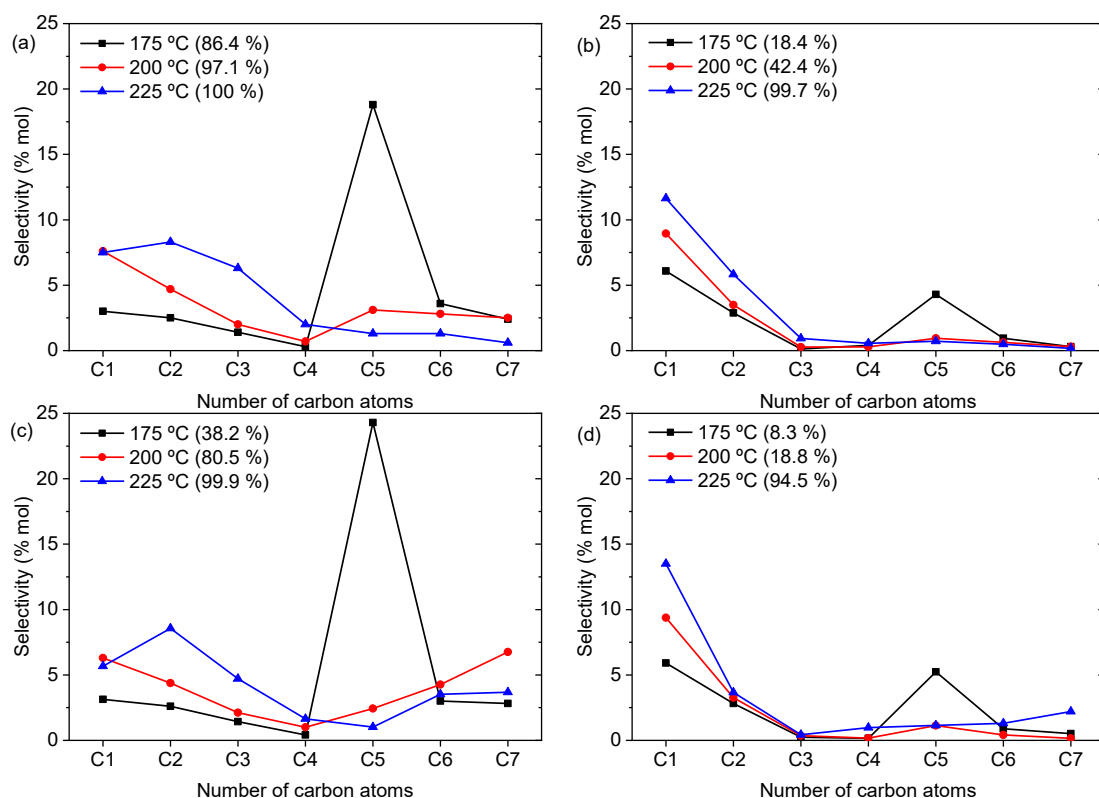


Figure 8. Selectivity towards C1 to C7 alkanes at different temperatures in APR of (a) 1 % maltose, (b) 1 % maltitol, (c) 2.5 % maltose and (d) 2.5 % maltitol. Numbers in brackets indicate conversion in the experiments at different temperatures (reaction conditions: 30 bar, 0.5 g of PtPd/C catalyst,  $WHSV = 0.12$  and  $0.3 \text{ h}^{-1}$ )

Figure 9 (a) shows the yield to  $\text{H}_2$  while Figure 9 (b) displays the turnover frequency for  $\text{H}_2$  production ( $TOF \text{ H}_2$ ) at different temperatures. Both  $\text{H}_2$  yield and  $TOF \text{ H}_2$  increased with reaction temperature and when less concentrated solutions were used. Under all tested operating conditions, the APR of maltitol always led to a higher  $\text{H}_2$  yield and  $TOF \text{ H}_2$  than the APR of maltose. In a former study on APR of glucose [9], the net production of  $\text{H}_2$  per mol of glucose was improved almost 3 fold by addition of a hydrogenation stage before reforming leading to sorbitol. In the current work, the  $\text{H}_2$  production was maximum for a reaction temperature of 225 °C and initial feedstock concentration of 1 %, resulting in a  $\text{H}_2$  yield and  $TOF \text{ H}_2$  for maltose of 26.4 % and  $0.29 \text{ min}^{-1}$ , respectively, while in the

APR of maltitol these values increased to 36.6 % and 0.42 min<sup>-1</sup>. Other authors found similar values of *TOF H<sub>2</sub>* in APR of polyols from glucose degradation (sorbitol, glycerol and ethylene glycol) using Pt/Al<sub>2</sub>O<sub>3</sub> catalyst (0.4-0.9 min<sup>-1</sup>) [26].

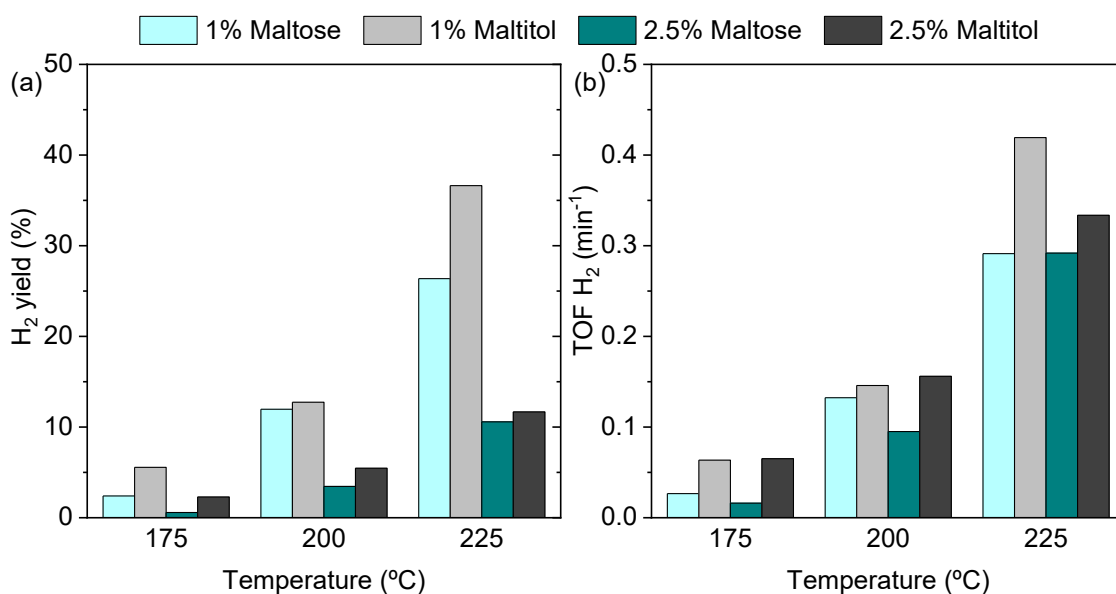


Figure 9. (a) H<sub>2</sub> yield and (b) *TOF H<sub>2</sub>* in the APR of maltose and maltitol at different temperatures and initial feedstock concentration (reaction conditions: 30 bar, 0.5 g of PtPd/C catalyst, *WHSV* = 0.12 and 0.3 h<sup>-1</sup>)

Arrhenius representations of the reaction rate for APR of 2.5 % maltose and maltitol, expressed as *TOF H<sub>2</sub>*, are shown in Figure 10. The apparent activation energies were 108 kJ/mol for APR of maltose and 61 kJ/mol for APR of maltitol. Comparison with the literature is not straightforward because no results have been reported so far for maltose and maltitol. However, the values are within the range of apparent activation energy found in the literature for the APR of glycerol (20 – 67 kJ/mol), methanol (140 kJ/mol) and ethylene glycol (100 kJ/mol) [27,28].

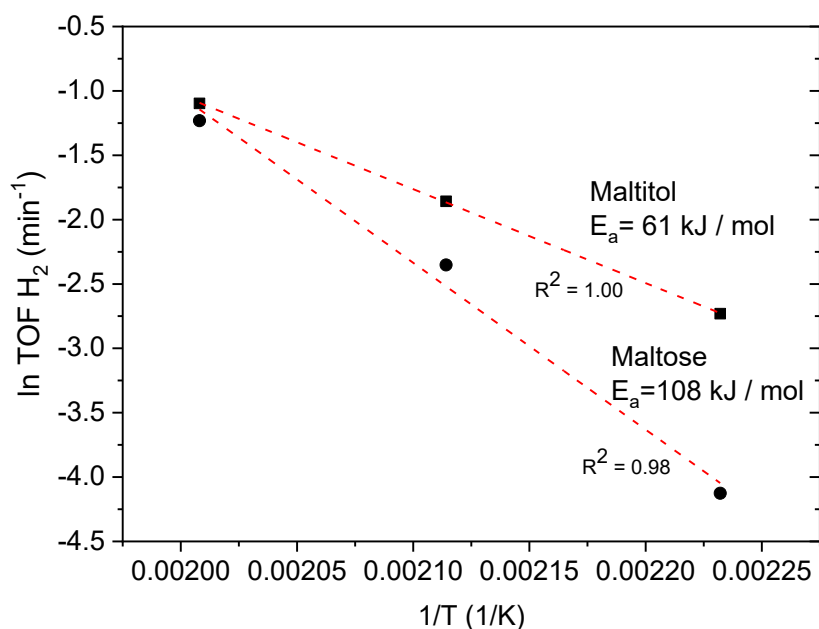


Figure 10. Arrhenius plot for APR of maltose and maltitol (reaction conditions: 30 bar, 2.5 % initial concentration, 0.5 g of PtPd/C catalyst,  $WHSV = 0.3 \text{ h}^{-1}$ )

Finally, in order to compare the catalytic performance in the APR of maltose and maltitol at similar conversion values, an additional experiment was performed at 200 °C using 2.5 % maltitol and  $WHSV$  of  $0.105 \text{ h}^{-1}$  (0.5 g of catalyst and 0.035 mL/min of flow rate). Table 1 shows the obtained results, also including for comparison the results for APR of maltose at the same temperature, initial solution concentration and  $WHSV$  of  $0.3 \text{ h}^{-1}$ . At a similar conversion level (74 – 80 %), the APR of maltitol yielded higher *CC gas* than APR of maltose. In addition, as observed previously, APR of maltose was more selective to alkanes production than APR of maltitol, while the selectivity to  $\text{H}_2$  was significantly higher in the APR of maltitol. Regarding the selectivity to C1-C7 alkanes, APR of maltitol was more selective to light alkanes, C1-C3 alkanes represented 75 % of the total alkanes selectivity, while APR of maltose was more selective to C4-C7 (53 % of the total alkanes selectivity). Furthermore, the selectivity to C1 was twice as high in the APR of maltitol than in the APR of maltose, whereas the selectivity to C7 was 17 times higher in the APR

of maltose. This high selectivity to C7 is indicative of the occurrence of condensation reactions [29], as otherwise C6 can be considered as the longest chain alkanes formed by dehydration/hydrogenation and/or dehydrogenation/decarbonylation [7]. The  $H_2$  yield and *TOF H<sub>2</sub>* were also higher in the APR of maltitol, highlighting that under these conditions the  $H_2$  yield increased from 3.4 to 12.4 %, evidencing the potential impact of a hydrogenation stage before APR.

Table 1. Results from APR of maltose and maltitol at similar conversion levels: 80.5 and 74.3 % correspondingly (200 °C, 2.5 % initial concentration, *WHSV* = 0.3 h<sup>-1</sup> maltose and 0.105 h<sup>-1</sup> maltitol)

	<b>Maltose</b>	<b>Maltitol</b>
<b>Conversion (%)</b>	80.5	74.3
<b>CC gas (%)</b>	15.5	24.5
<b>H<sub>2</sub> selectivity (%)</b>	53.2	71.7
<b>CO<sub>2</sub> selectivity (%)</b>	72.7	76.1
<b>Alkanes selectivity (%)</b>	27.3	23.9
<b>Selectivity (%)</b>		
C1	6.3	12.2
C2	4.4	5.1
C3	2.1	0.7
C4	1.0	0.5
C5	2.4	4.3
C6	4.3	0.7
C7	6.8	0.4
<b>H<sub>2</sub> yield (%)</b>	3.4	12.4
<b>TOF H<sub>2</sub> (min<sup>-1</sup>)</b>	0.10	0.12

### 3.2.3. Liquid phase composition

The liquid phase resulting from APR at different temperatures was analysed by HPLC to identify the main reaction products and to obtain insight into the reaction mechanism. Figure 11 shows the HPLC chromatograms for reactions at 175 °C, 200 °C and 225 °C. Zoomed inserts in the Figure 11 (b), (c) and (d) illustrate the ratio between major and minor peaks. The compounds identified are similar to those observed in the liquid phase

of APR of other feedstocks such as sorbitol, galactitol, glycerol or xylitol [23,29–31] and in the degradation of carbohydrates at high temperatures [32–34].

The chromatograms in Figure 11 show significantly different patterns for maltose and maltitol. In the APR of maltose, glucose (3) and fructose (5) were identified, especially at 175 °C. The occurrence of glucose can be ascribed to hydrolysis of maltose in the acidic medium or on acidic sites of the catalyst [35], while fructose can result from isomerization of glucose, which is promoted by the presence of Pt catalyst and H<sub>2</sub> [36]. In the APR of maltitol, sorbitol (7) was identified, especially at 225 °C, whereas glucose (3) and fructose (5) were not detected. Sorbitol can be produced by hydrolysis of maltitol [18] and hydrogenation of glucose and fructose [37], thus a high peak observed for sorbitol at a high temperature reaction (225 °C) is consistent with the decrease in H<sub>2</sub> selectivity observed in the APR of maltitol at this temperature. On the other hand, the route of hydrogenation of glucose and fructose does not seem to be favoured in the APR of maltose, since sorbitol was not detected in the liquid phase for this substrate.

In addition to the sugars/sugar alcohols, a number of aldehydes, organic acids and alcohols were identified in the APR of both maltose and maltitol, while glycolaldehyde (11), propylene glycol (19) and methanol (22) were only detected in the APR of maltitol and pyruvaldehyde (10), formic acid (15) and levulinic acid (18) were only detected in the APR of maltose. In addition, HMF (not shown, 35.5 min) was also only detected in the APR of maltose at 200 °C.

Regarding the distribution of the liquid products, the concentration of the compounds detected are included in Supplementary Material (Table S1 and S2). In the APR of maltose at 175 °C, glucose (3), formic acid (15), hydroxyacetone (20) and ethanol (24) yielded the main concentrations, representing between 12.7 and 21.3 % of the starting carbon. At 200 °C and using 1 % maltose, hydroxyacetone (20) and ethanol (24) obtained



1 the highest concentrations, representing 22.6 % of the starting carbon, while using 2.5 %  
2 initial solution, the main concentrations correspond to glucose (3) and ethanol (24), with  
3 14.1 % of the starting carbon. On the other hand, at 225 °C, the APR of maltose yielded  
4 mainly ethanol (24), representing between 1.1 and 1.9 % of the starting carbon. It is  
5 important to note that the high concentrations of ethanol observed at higher reaction  
6 temperatures are consistent with the increase in selectivity to C2 observed above.

7 In the APR of maltitol at 175 and 200 °C, the main compounds are glyceraldehyde (8),  
8 hydroxyacetone (20) and methanol (22), representing between 2.6 and 4 % of the starting  
9 carbon. At 225 °C and using 1% maltitol, acetaldehyde (21), methanol (22) and ethanol  
10 (24) yielded the main concentrations, representing 13.8 % of the starting carbon, while  
11 using 2.5 % maltitol, sorbitol (7) was the main compound produced, with 29.3 % of the  
12 starting carbon, followed by hydroxyacetone (20), with 11.4 % of the starting carbon. The  
13 high concentration of hydroxyacetone and acetaldehyde observed are related to the high  
14 selectivity to C1 observed in the APR of maltitol [30].

15 Regarding the influence of reaction temperature, C-C and C-O bond cleavage are  
16 favoured by increasing the reaction temperature [23], leading to products with less carbon  
17 atoms in the liquid phase and higher *CC gas*. In this sense, a higher concentration of  
18 hydroxyacetone (20), acetaldehyde (21) and ethanol (24) was observed at 200 and 225  
19 °C, also in agreement with the increase in the selectivity to C1-C2 alkanes [30]

20 Taking into account the obtained results, the degradation of maltose may proceed mainly  
21 *via* hydrolysis generating glucose, which in turn leads to HMF by dehydration, becoming  
22 a precursor of formic and levulinic acids [38]. This route also generates compounds that  
23 could be related to the production of C5 alkanes, such as pentanol and 1,5-pentanediol  
24 [5], consistent with the higher C5 selectivity observed in the APR of maltose. On the  
25 other hand, degradation route of maltitol may proceed mainly *via* hydrolysis generating

1 sorbitol and glucose [18]. Sorbitol undergoes reforming to produce  $H_2$  that also is used in  
2 sequential dehydration-hydrogenation steps which together with decarbonylation  
3 reactions, leading to ketones, aldehydes, acids and alcohols and then alkanes [9]. In this  
4 context, Kirilin et al. [23] found that the selectivity to light alkanes (C1-C3) was higher  
5 than C4-C6 alkanes in the APR of sorbitol at the same *WHSV*, consistent with high  
6 selectivities to C1-C2 alkanes observed in the APR of maltitol. Other possible parallel  
7 routes could be the retro-aldol fragmentation of glucose and/or fructose [5]. These routes  
8 could also occur because they lead to the formation of various liquid compounds  
9 identified in this work, such as glycolaldehyde, glyceraldehyde, acetaldehyde,  
10 hydroxyacetone, ethanol and methanol.

11 Finally, some of the liquid phase compounds that were detected only in the APR of  
12 maltose (glucose, fructose, pyruvaldehyde, HMF) are known to be relevant precursors in  
13 solid humins formation during the catalytic hydrothermal conversion of carbohydrates  
14 [39]. This contribution may be much lower in the APR of maltitol, where a different  
15 pattern in liquid phase products distribution was found, evidencing differences in the  
16 degradation routes.

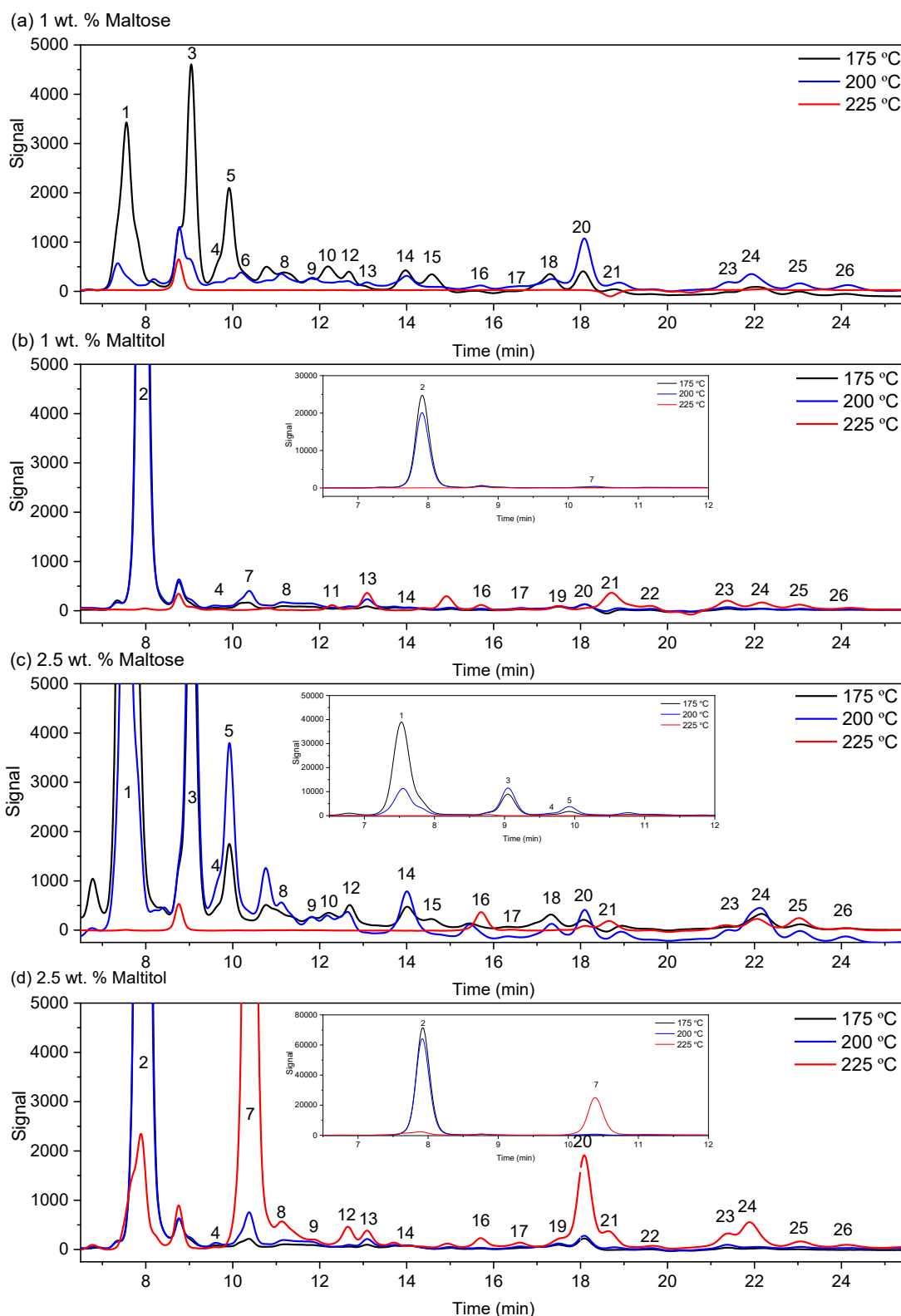


Figure 11. HPLC chromatograms of the liquid samples during APR of maltose and maltitol at different temperatures and initial feedstock concentrations. Identified compounds: (1) maltose, (2) maltitol, (3) glucose, (4) xylose, (5) fructose, (6) mannitol, (7) sorbitol, (8) glyceraldehyde, (9) erythritol, (10) pyruvaldehyde, (11) glycolaldehyde, (12) glycolic acid, (13) lactic acid, (14) formaldehyde, (15) formic acid, (16) acetic acid, (17) ethylene glycol, (18) levulinic acid, (19) propylene glycol, (20) hydroxyacetone, (21)

acetaldehyde, (22) methanol, (23) 1-2 butanediol, (24) ethanol, (25) butyric acid and (26) isopropanol (reaction conditions: 30 bar, 0.5 g of PtPd/C catalyst,  $WHSV = 0.12$  and  $0.3 \text{ h}^{-1}$ )

The comparative data obtained in the APR of maltose and maltitol at similar conversion levels revealed significant differences in the composition of the liquid phase, with higher yield to sugars, sugar alcohols, alcohols, acids, aldehydes and ketones, and occurrence of HMF in the APR of maltose (Table 2). Accordingly, the total carbon present in the liquid phase was higher in the APR of maltose.

Table 2. Yields of the liquid phase products obtained during APR of maltose and maltitol (200 °C, 2.5 % initial concentration,  $WHSV = 0.3 \text{ h}^{-1}$  maltose and  $0.105 \text{ h}^{-1}$  maltitol)

	<b>Maltose</b>	<b>Maltitol</b>
<b>Conversion (%)</b>	80.5	74.3
<b>Yield to product (%)</b>		
<b>sugar/sugar alcohol</b>		
glucose	10.2	-
xylose	0.5	0.3
fructose	4.7	-
sorbitol	-	0.6
erythritol	1.0	<0.1
<b>alcohols</b>		
ethylene glycol	0.5	0.2
propylene glycol	-	<0.1
methanol	-	0.6
1-2 butanediol	1.0	1.0
ethanol	3.9	2.5
isopropanol	1.2	0.1
<b>acids</b>		
glycolic acid	2.1	0.2
lactic acid	-	0.7
acetic acid	0.2	0.2
levulinic acid	2.2	-
butyric acid	1.6	0.2
<b>aldehydes/ketones</b>		
glyceraldehyde	2.9	2.3
pyruvaldehyde	0.6	-
formaldehyde	1.1	<0.1
hydroxyacetone	3.9	0.8
acetaldehyde	-	2.4
<b>furans</b>		

HMF	0.4	-
<b>Total yield to identified products</b>	38.0	12.2
<b>Total carbon in liquid phase (%)*</b>	57.4	37.9

\*: calculated from identified products, carbon in the initial feedstock

#### 3.2.4. Carbon Balance

The carbon mass balance closure was higher in the maltitol APR experiments (91 to 100 %) than for those with maltose (56 to 95 %). In addition, a higher carbon imbalance was observed for high reaction temperatures with a higher feedstock concentration, especially in the case of APR experiments with maltose, where 44 % of carbon was not detected either in the liquid phase or in the gas phase. In the literature [2], the solid phase production was found to increase with the initial concentration of the feedstock in APR of glucose and xylose, which was attributed to formation of high molecular weight compounds by condensation reactions. Therefore, deposition of the solid phase mater is consistent with the lower mass balance closure for APR of maltose.

Considering that the undetected carbon is present in the reaction as solid phase carbon species, diagrams of the carbon distribution between gas, liquid and solid phases in the APR experiments are shown in Figure 12. It can be seen from these diagrams that the estimated fraction of carbon in the solid phase is higher in the APR of maltose compared with maltitol, even at the same feedstock conversion, and that deposition of the solid carbon can be responsible for faster deactivation and collapse of the flow due to a high pressure drop. It can be also observed that, in the APR of maltose, the increase of solid phase formation occurs at the expense of liquid phase species formation to a higher extent than in the APR of maltitol.

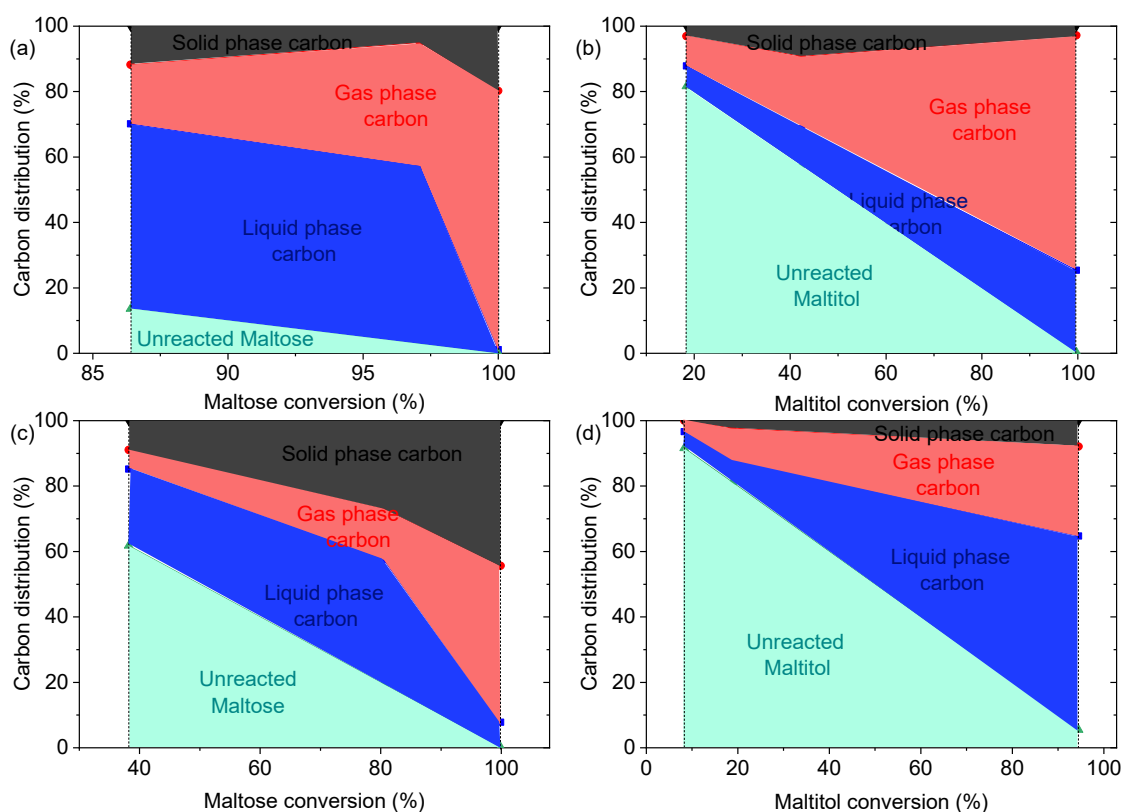


Figure 12. Carbon distribution in APR of (a) 1 % maltose, (b) 1 % maltitol, (c) 2.5 % maltose and (d) 2.5 % maltitol (reaction conditions: 175, 200 and 225 °C, 30 bar, 0.5 g of PtPd/C catalyst,  $WHSV = 0.12$  and  $0.3 \text{ h}^{-1}$ )

In order to evaluate formation of the solid phase carbon species during APR experiments, the used catalysts were subjected to TG-TPD/TPO tests. Figure 13 shows the weight-loss TG-TPD/TPO profiles and the corresponding differential curves (DTG) for the PtPd/C catalyst used in the APR of 1 % maltose and maltitol and 2.5 % maltose. The quantitative values of the weight loss are summarized in Table 3.

The initial peak at ca. 100 °C in TG-TPD curves can be ascribed to the loss of water. After that, the used catalysts, especially the one employed in the case of 2.5% maltose, showed a peak extending from 200 to 425 °C, which can be attributed to the loss of carbon-rich (coke-like) species or reactants/products physically adsorbed on the catalyst. The

percentage of the weight loss in the TG-TPD was 2.4 % in the case of the catalyst used in APR of 1% maltitol, and increased to 4.7 and 10.4 % for the APR of 1 % and 2.5 % maltose, respectively (Table 3). Therefore, during the APR of maltose higher amounts of carbon-rich species are deposited on the catalyst, and their desorption and evolution under pyrolysis lead to a higher loss weight in TG-TPR tests. Regarding the TG-TPO profiles, the displacement of the main peak towards higher combustion temperatures suggest a higher degree of structure development for the carbon-rich species deposited during upon APR of maltose. It should be also noted that TG-TPO tests are carried out subsequently to TG-TPD ones, then part of the mass oxidized during TPO can be ascribed to the carbonizate resulting from the pyrolysis of carbon-rich species during TPD. Therefore, the results obtained allow considering formation of the solid phase carbon species as a reason of catalyst deactivation observed in the APR of maltose compared to maltitol.

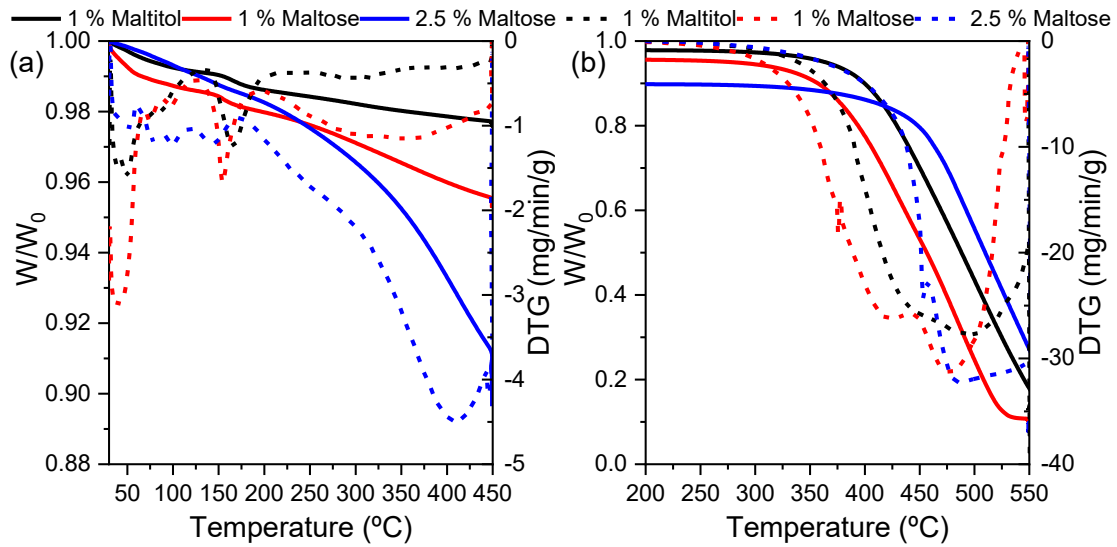


Figure 13. (a) TG-TPD and (b) TG-TPO profiles and the corresponding derivative curves of the spent PtPd/C catalysts (reaction conditions: 175, 200 and 225 °C, 30 bar, 0.5 g of PtPd/C catalyst,  $WHSV = 0.12$  and  $0.3 \text{ h}^{-1}$ )

Table 3. Quantitative weight losses upon TG-TPD/TPO of used catalysts (reaction conditions: 175, 200 and 225 °C, 30 bar, 0.5 g of PtPd/C catalyst,  $WHSV = 0.12$  and  $0.3 \text{ h}^{-1}$ )

Catalyst	TG-TPD (%)	TG-TPO (%)
Used in APR of 1 % Maltitol	2.4	84.9
Used in APR of 1 % Maltose	4.7	85.0
Used in APR of 2.5 % Maltose	10.4	81.8

### 3.2.5. Process efficiency

Regarding efficiency of the overall coupled hydrogenation and APR process, it has to be considered that 1 mol of  $\text{H}_2$  is utilized to hydrogenate 1 mol of maltose to maltitol (Equation 8). On the other hand, considering the global APR reactions in Equations 9 and 10, the maximum  $\text{H}_2$  production from 1 mol maltose and maltitol is 24 and 25 mol, respectively. Therefore, the coupled process could be considered efficient if leads to a more stable conditions for PtPd/C catalyst performance despite a certain amount of  $\text{H}_2$  needed in the hydrogenation step.



As mentioned above, because the apparent activation energy for  $\text{H}_2$  production is lower in the APR of maltitol than in the APR of maltose, selectivity for  $\text{H}_2$  production was higher, ultimately increasing  $\text{H}_2$  yield in the coupled process. At 225 °C the APR of 1 % maltose generated 6.3 mol of  $\text{H}_2$  per mol of maltose, while 9.2 mol of  $\text{H}_2$  was produced in the APR of maltitol. Thus, introduction of a hydrogenation stage before APR generated 3 additional moles of  $\text{H}_2$  than direct reforming of maltose. Therefore, the overall process could be considered efficient under these conditions. For 2.5 % feedstock the production



of H<sub>2</sub> from maltose and maltitol was 2.5 and 2.9 mol per mol of the feedstock, respectively, not covering the needs for hydrogenation. At the same time, hydrogenation to maltitol had a clear impact on catalyst durability, contributing to the efficiency and feasibility of the process. In the view of these results, an alternative approach could be hydrogenation of maltose to such products as sorbitol [40,41], which can result in a higher H<sub>2</sub> yield in subsequent APR [9,31]. The results also show a potential of APR of the diluted feedstock in terms of a high conversion of substrate and selectivity to H<sub>2</sub>.

#### 4. Conclusions

Hydrogenation of maltose to maltitol was performed as a pre-stage of APR to increase overall H<sub>2</sub> production and diminish the deactivation by formation of carbonaceous deposits. Maltose was selected as a model compound because it is the main component present in brewery wastewaters, which has a large potential for valorisation.

In the APR of maltose after 48 h TOS and at 225 °C, a significant catalyst deactivation and increase of the pressure in the reactor was observed, probably due to formation of carbonaceous deposits on the catalyst surface and on the walls of the reactor. In contrast, in the APR of maltitol lower deactivation was observed, indicating that undesirable reactions that take place in the liquid phase to form carbonaceous deposits are less favoured. High feedstock concentration also contributed to deactivation, particularly at a high reaction temperature.

Conversion of the initial feedstock and carbon conversion to gas phase were higher in the APR of maltose, however, higher H<sub>2</sub> selectivity was achieved in the combined hydrogenation and APR. In addition, conversion of the substrate and H<sub>2</sub> selectivity were

significantly higher at a low feedstock concentration, showing the potential of diluted streams and wastewaters.

APR of maltose was more selective to alkanes than APR of maltitol, and both feedstocks led to a remarkably high selectivity to C<sub>5</sub> at 175 °C. At 225 °C the APR of maltose was more selective to C<sub>2</sub> while the APR of maltitol was more selective to C<sub>1</sub>. In the liquid phase, higher yields of sugar, sugar alcohols, alcohols, acids, aldehydes and ketones were obtained in the APR of maltose. Both H<sub>2</sub> yield and *TOF* H<sub>2</sub> were higher for a high reaction temperature and less concentrated feedstocks. In addition, the APR of maltitol always led to a higher H<sub>2</sub> yield and *TOF* H<sub>2</sub> than the APR of maltose, and the value of apparent activation energy calculated was lower for APR of maltitol (61 kJ/mol) than in the APR of maltose (108 kJ/mol).

Finally, the overall process (combined hydrogenation and APR) can be considered as efficient because an increase in H<sub>2</sub> production compensated for the consumption in hydrogenation, and moreover durability of the catalyst was increased in the APR of maltitol.

## Acknowledgements

The authors greatly appreciate financial support from Spanish MINECO (CTQ2015-65491-R). A. S. Oliveira is grateful to the Spanish MINECO for a research grant (BES-2016-077244). Synthesis of PtPd on Sibunit catalyst was supported by RFBR Grant 18-53-45013 IND\_a.

1

## 2   **References**

- 3   [1]   R.D. Cortright, R.R. Davda, J.A. Dumesic, Hydrogen from catalytic reforming of  
4       biomass-derived hydrocarbons in liquid water, *Nature*. 418 (2002) 964–967.  
5       doi:10.1038/nature01009.
- 6   [2]   G. Pipitone, G. Zoppi, A. Frattini, S. Bocchini, R. Pirone, S. Bensaid, Aqueous  
7       phase reforming of sugar-based biorefinery streams: from the simplicity of model  
8       compounds to the complexity of real feeds, *Catal. Today*. 345 (2020) 267–279.  
9       doi:10.1016/j.cattod.2019.09.031.
- 10   [3]   A. Aho, C. Rosales, K. Eränen, T. Salmi, D.Y. Murzin, H. Grénman, Biohydrogen  
11       from dilute side streams - Influence of reaction conditions on the conversion and  
12       selectivity in aqueous phase reforming of xylitol, *Biomass and Bioenergy*. 138  
13       (2020) 105590. doi:10.1016/j.biombioe.2020.105590.
- 14   [4]   A.S. Oliveira, J.A. Baeza, L. Calvo, N. Alonso-Morales, F. Heras, J.J. Rodriguez,  
15       M.A. Gilarranz, Production of hydrogen from brewery wastewater by aqueous  
16       phase reforming with Pt/C catalysts, *Appl. Catal. B Environ*. 245 (2019) 367–375.  
17       doi:10.1016/j.apcatb.2018.12.061.
- 18   [5]   J. Remón, J. Ruiz, M. Oliva, L. García, J. Arauzo, Cheese whey valorisation:  
19       Production of valuable gaseous and liquid chemicals from lactose by aqueous  
20       phase reforming, *Energy Convers. Manag.* 124 (2016) 453–469.  
21       doi:10.1016/j.enconman.2016.07.044.
- 22   [6]   B. Saenz de Miera, A.S. Oliveira, J.A. Baeza, L. Calvo, J.J. Rodriguez, M.A.  
23       Gilarranz, Treatment and valorisation of fruit juice wastewater by aqueous phase

reforming: Effect of pH, organic load and salinity, *J. Clean. Prod.* 252 (2020) 119849. doi:10.1016/J.JCLEPRO.2019.119849.

[7] D.A. Sladkovskiy, L.I. Godina, K. V. Semikin, E. V. Sladkovskaya, D.A. Smirnova, D.Y. Murzin, Process design and techno-economical analysis of hydrogen production by aqueous phase reforming of sorbitol, *Chem. Eng. Res. Des.* 134 (2018) 104–116. doi:10.1016/j.cherd.2018.03.041.

[8] R.R. Davda, J.W. Shabaker, G.W. Huber, R.D. Cortright, J.A. Dumesic, A review of catalytic issues and process conditions for renewable hydrogen and alkanes by aqueous-phase reforming of oxygenated hydrocarbons over supported metal catalysts, *Appl. Catal. B Environ.* 56 (2005) 171–186. doi:10.1016/j.apcatb.2004.04.027.

[9] R.R. Davda, J.A. Dumesic, Renewable hydrogen by aqueous-phase reforming of glucose, *Chem. Commun.* 10 (2004) 36–37. doi:10.1002/anie.200353050.

[10] R. V. Stick, S.J. Williams, *Carbohydrates: The Essential Molecules of Life*, 2nd Editio, Elsevier, 2009. doi:10.1016/B978-0-240-52118-3.X0001-4.

[11] S. Irmak, B. Meryemoglu, A. Hasanoglu, O. Erbatur, Does reduced or non-reduced biomass feed produce more gas in aqueous-phase reforming process?, *Fuel*. 139 (2015) 160–163. doi:10.1016/J.FUEL.2014.08.028.

[12] L.I. Godina, H. Heeres, S. Garcia, S. Bennett, S. Poulston, D.Y. Murzin, Hydrogen production from sucrose via aqueous-phase reforming, *Int. J. Hydrogen Energy*. 44 (2019) 14605–14623. doi:10.1016/j.ijhydene.2019.04.123.

[13] H. Habte Lemji, H. Eckstädt, A pilot scale trickling filter with pebble gravel as media and its performance to remove chemical oxygen demand from synthetic

- 1 brewery wastewater, *J Zhejiang Univ-Sci B (Biomed & Biotechnol)*. 14 (2013)
- 2 924–933. doi:10.1631/jzus.B1300057.
- 3 [14] G.S. Simate, J. Cluett, S.E. Iyuke, E.T. Musapatika, S. Ndlovu, L.F. Walubita, A.E.
- 4 Alvarez, The treatment of brewery wastewater for reuse: State of the art,
- 5 *Desalination*. 273 (2011) 235–247. doi:10.1016/j.desal.2011.02.035.
- 6 [15] M.K. Arantes, H.J. Alves, R. Sequinel, E.A. da Silva, Treatment of brewery
- 7 wastewater and its use for biological production of methane and hydrogen, *Int. J.*
- 8 *Hydrogen Energy*. 42 (2017) 26243–26256. doi:10.1016/j.ijhydene.2017.08.206.
- 9 [16] R.R. Davda, J.W. Shabaker, G.W. Huber, R.D. Cortright, J.A. Dumesic, Aqueous-
- 10 phase reforming of ethylene glycol on silica-supported metal catalysts, *Appl.*
- 11 *Catal. B Environ*. 43 (2003) 13–26. doi:10.1016/S0926-3373(02)00277-1.
- 12 [17] C. He, J. Zheng, K. Wang, H. Lin, J.-Y. Wang, Y. Yang, Sorption enhanced
- 13 aqueous phase reforming of glycerol for hydrogen production over Pt-Ni supported
- 14 on multi-walled carbon nanotubes, *Appl. Catal. B Environ*. 162 (2015) 401–411.
- 15 doi:10.1016/j.apcatb.2014.07.012.
- 16 [18] E.M. Sulman, M.E. Grigorev, V.Y. Doluda, J. Wärnå, V.G. Matveeva, T. Salmi,
- 17 D.Y. Murzin, Maltose hydrogenation over ruthenium nanoparticles impregnated in
- 18 hypercrosslinked polystyrene, *Chem. Eng. J*. 282 (2015) 37–44.
- 19 doi:10.1016/j.cej.2015.04.002.
- 20 [19] A. Aho, S. Roggan, O.A. Simakova, T. Salmi, D.Y. Murzin, Structure sensitivity
- 21 in catalytic hydrogenation of glucose over ruthenium, *Catal. Today*. 241 (2015)
- 22 195–199. doi:10.1016/j.cattod.2013.12.031.
- 23 [20] L.I. Godina, A. V. Kirilin, A. V. Tokarev, I.L. Simakova, D.Y. Murzin, Sibunit-

- supported mono- and bimetallic catalysts used in aqueous-phase reforming of xylitol, *Ind. Eng. Chem. Res.* 57 (2018) 2050–2067. doi:10.1021/acs.iecr.7b04937.
- [21] A. V. Kirilin, B. Hasse, A. V. Tokarev, L.M. Kustov, G.N. Baeva, G.O. Bragina, A.Y. Stakheev, A.-R. Rautio, T. Salmi, B.J.M. Etzold, J.-P. Mikkola, D.Y. Murzin, Aqueous-phase reforming of xylitol over Pt/C and Pt/TiC-CDC catalysts: catalyst characterization and catalytic performance, *Catal. Sci. Technol.* 4 (2014) 387–401. doi:10.1039/C3CY00636K.
- [22] J. Song, H. Fan, J. Ma, B. Han, Conversion of glucose and cellulose into value-added products in water and ionic liquids, *Green Chem.* 15 (2013) 2619–2635. doi:10.1039/c3gc41141a.
- [23] A. V. Kirilin, A. V. Tokarev, E. V. Murzina, L.M. Kustov, J.P. Mikkola, D.Y. Murzin, Reaction products and transformations of intermediates in the aqueous-phase reforming of sorbitol, *ChemSusChem.* 3 (2010) 708–718. doi:10.1002/cssc.200900254.
- [24] M. Alvear, A. Aho, I.L. Simakova, H. Grénman, T. Salmi, D.Y. Murzin, Aqueous phase reforming of alcohols over a bimetallic Pt-Pd catalyst in the presence of formic acid, *Chem. Eng. J.* 398 (2020) 125541. doi:10.1016/j.cej.2020.125541.
- [25] G.W. Huber, R.D. Cortright, J.A. Dumesic, Renewable alkanes by aqueous-phase reforming of biomass-derived oxygenates, *Angew. Chemie - Int. Ed.* 43 (2004) 1549–1551. doi:10.1002/anie.200353050.
- [26] L.A. Dosso, C.R. Vera, J.M. Grau, Aqueous phase reforming of polyols from glucose degradation by reaction over Pt/alumina catalysts modified by Ni or Co, *Int. J. Hydrogen Energy.* 42 (2017) 18853–18864. doi:10.1016/j.ijhydene.2017.06.100.

- [27] J.W. Shabaker, R.R. Davda, G.W. Huber, R.D. Cortright, J.A. Dumesic, Aqueous-phase reforming of methanol and ethylene glycol over alumina-supported platinum catalysts, *J. Catal.* 215 (2003) 344–352. doi:10.1016/S0021-9517(03)00032-0.
- [28] F.J. Gutiérrez Ortiz, F.J. Campanario, P. Ollero, Turnover rates for the supercritical water reforming of glycerol on supported Ni and Ru catalysts, *Fuel*. 180 (2016) 417–423. doi:10.1016/J.FUEL.2016.04.065.
- [29] L.I. Godina, A. V. Kirilin, A. V. Tokarev, D.Y. Murzin, Aqueous phase reforming of industrially relevant sugar alcohols with different chiralities, *ACS Catal.* 5 (2015) 2989–3005. doi:10.1021/cs501894e.
- [30] L.I. Godina, A. V. Tokarev, I.L. Simakova, P. Mäki-Arvela, E. Kortesmäki, J. Gläsel, L. Kronberg, B. Etzold, D.Y. Murzin, Aqueous-phase reforming of alcohols with three carbon atoms on carbon-supported Pt, *Catal. Today*. 301 (2018) 78–89. doi:10.1016/j.cattod.2017.03.042.
- [31] A. V. Kirilin, A. V. Tokarev, L.M. Kustov, T. Salmi, J.-P. Mikkola, D.Y. Murzin, Aqueous phase reforming of xylitol and sorbitol: Comparison and influence of substrate structure, *Appl. Catal. A Gen.* 435–436 (2012) 172–180. doi:10.1016/j.apcata.2012.05.050.
- [32] B.M. Kabyemela, T. Adschiri, R.M. Malaluan, K. Arai, Glucose and fructose decomposition in subcritical and supercritical water: detailed reaction pathway, mechanisms, and kinetics, *Ind. Eng. Chem. Res.* 38 (1999) 2888–2895. doi:10.1021/ie9806390.
- [33] M. Bicker, S. Endres, L. Ott, H. Vogel, Catalytical conversion of carbohydrates in subcritical water: A new chemical process for lactic acid production, *J. Mol. Catal. A Chem.* 239 (2005) 151–157. doi:10.1016/J.MOLCATA.2005.06.017.

- 1 [34] A. Sınağ, S. Gülbay, B. Uskan, M. Canel, Biomass decomposition in near critical  
2 water, Energy Convers. Manag. 51 (2010) 612–620.  
3 doi:10.1016/J.ENCONMAN.2009.11.009.
- 4 [35] A. Abbadi, K.F. Gotlieb, H. van Bekkum, Study on solid acid catalyzed hydrolysis  
5 of maltose and related polysaccharides, Starch - Stärke. 50 (1998) 23–28.  
6 doi:10.1002/(SICI)1521-379X(199801)50:1<23::AID-STAR23>3.3.CO;2-K.
- 7 [36] Y. Kanie, K. Akiyama, M. Iwamoto, Reaction pathways of glucose and fructose  
8 on Pt nanoparticles in subcritical water under a hydrogen atmosphere, Catal.  
9 Today. 178 (2011) 58–63. doi:10.1016/J.CATTOD.2011.07.031.
- 10 [37] M.J. Ahmed, B.H. Hameed, Hydrogenation of glucose and fructose into hexitols  
11 over heterogeneous catalysts: A review, J. Taiwan Inst. Chem. Eng. 96 (2019)  
12 341–352. doi:10.1016/J.JTICE.2018.11.028.
- 13 [38] J.N. Chheda, G.W. Huber, J.A. Dumesic, Liquid-phase catalytic processing of  
14 biomass-derived oxygenated hydrocarbons to fuels and chemicals, Angew.  
15 Chemie - Int. Ed. 46 (2007) 7164–7183. doi:10.1002/anie.200604274.
- 16 [39] N. Shi, Q. Liu, R. Ju, X. He, Y. Zhang, S. Tang, L. Ma, Condensation of  $\alpha$ -carbonyl  
17 aldehydes leads to the formation of solid humins during the hydrothermal  
18 degradation of carbohydrates, ACS Omega. 4 (2019) 7330–7343.  
19 doi:10.1021/acsomega.9b00508.
- 20 [40] J. Zhang, J. Li, S. Wu, Y. Liu, Efficient conversion of maltose into sorbitol over  
21 magnetic catalyst in extremely low acid, BioResources. 8 (2013) 4676–4686.  
22 doi:10.15376/biores.8.3.4676-4686.
- 23 [41] L. Negahdar, P.J.C. Hausoul, S. Palkovits, R. Palkovits, Direct cleavage of sorbitol



- 1 from oligosaccharides via a sequential hydrogenation-hydrolysis pathway, *Appl.*
- 2 *Catal. B Environ.* 166–167 (2015) 460–464. doi:10.1016/J.APCATB.2014.11.049.
- 3